Wireless Pers Commun (2017) 96:291–302
DOI 10.1007/s11277-017-4167-6

An Efficient Source–Channel Coding for Wireless Image Transmission Over Underwater Acoustic Channel

Hanaa S. Ali[1] · **Asmaa M. Atallah**[1,2] · **M. I. Abdalla**[1]

Published online: 3 May 2017

Abstract In this paper, a complete system for image transmission in harsh underwater environment is proposed. The key to increase the performance of the system is the use of an efficient image compression algorithm with a bandwidth-efficient modulation technique. The wavelet packet (WP) decomposition is used to get the best image representation and the set partitioning in hierarchical trees is applied on the WP coefficients. The parental conflicts are resolved, the parent–child relationships are adapted and thus the similarities between cross-subbands are preserved. Reed–Solomon is used for forward error correction to combat with the errors in wireless transmission. Orthogonal frequency division multiplexing with differential quadrature phase shift keying is used to transmit the generated bit stream. Effective image quality metrics are used for objective evaluation. Results show that the proposed system manages to transmit images over the limited bandwidth, and to effectively minimize the perceptual degradation.

Keywords Wavelet packets · Underwater wireless channel · Image compression · SPIHT · OFDM · Reed–Solomon

✉ Hanaa S. Ali
hanahshaker@yahoo.com

Asmaa M. Atallah
asmaa.atalla@yahoo.com

M. I. Abdalla
mabdalla2010@gmail.com

[1] Electronics & Communication Dept., Faculty of Engineering, Zagazig University, Zagazig, Egypt

[2] Zagazig Higher Institute for Engineering and technology, Zagazig, Egypt

1 Introduction

Efficient technologies for underwater wireless transmission are desirable to facilitate ocean exploration and monitoring. The conversion of the technology from terrestrial to underwater links is difficult, since the channel parameters are radically different. The speed of the acoustic waves is much lower and the path loss is higher. Moreover, the bandwidth is limited, and thus limited data rates can be accommodated [1–4]. To avoid these limitations, two aspects should be taken into consideration: efficient compression technique and bandwidth efficient modulation. Compression enables transmission at a much lower bit rate. Orthogonal frequency division multiplexing efficiently uses the limited bandwidth and can combat the multipath propagation problem using less complex receivers [5].

The interest in exploring the underwater environment especially with image transmission has been increasing. In [6], error concealment and error correction algorithms are applied for quality-aware image transmission over underwater channel. In [7], OFDM with binary phase shift keying (BPSK) is used for underwater image transmission. Least square (LS) and minimum mean square error (MMSE) are used for equalization. Tomasi et al. [8] propose a system for transmitting encoded image and use forward error correction (FEC) for symbols protection. The multiple descriptions (MD) technique results in performance improvement compared to the basic allocation one. Ismaiel and Jiang [2] propose a system for SPIHT-based image transmission. Hierarchical quadrature amplitude modulation (16-HQAM) and Reed–Solomon (RS) are used to reduce the bit error rate using an unequal protection mechanism. Decision feedback equalizers (DFEs) are used to equalize the received data. In [4], they propose an OFDM system in which RS is used with HQAM to reduce bit error without using an equalizer. In [9], they propose a rate allocation scheme with SPIHT-based compression for performance improvement.

In this paper, an efficient source–channel coding is introduced to transmit images over underwater wireless channel. The target is reducing the bit error rate (BER) due to channel impairments, and reconstructing the images with high visual quality at the receiver. SPIHT algorithm is applied on WP coefficients. The spatial orientation trees (SOT_s) are adapted to maintain the cross-subband similarities. For burst error correction, RS codes are used. OFDM is used in the proposed system to handle multipaths and to avoid complex channel equalization. DQPSK is used to avoid complex carrier tracking. To predict the quality of the received image, effective metrics are used. Multi-scale structural similarity index (MS-SSIM) is employed. It takes advantage of the human visual system characteristics, and can incorporate the details of the image at different levels. The peak signal-to-noise ratio (PSNR) and the weighted peak signal-to-noise ratio (WPSNR) are also used.

The rest of the paper is organized as follows: The underwater channel model is presented in Sect. 2. The proposed system is introduced in Sect. 3. Simulation setup and results are presented in Sect. 4. The paper is concluded in Sect. 5.

2 Underwater Acoustic Channel

The overall attenuation loss in underwater acoustic channel is given by [6, 10]

$$A(d,f) = d^k a(f)^d \tag{1}$$

where d is the distance between the transmitter and receiver, f is the signal frequency and k is the spreading coefficient. A value of $k = 1.5$ is usually used. The absorption loss $a(f)$

results from the conversion of acoustic energy into heat. This absorption is proportional to the frequency squared and thus causes a frequency selective channel fading:

$$A(f) = \frac{0.11f^2}{1+f^2} + \frac{40f^2}{4100+f^2} + 2.75 \times 10^{-4} f^2 + 0.003 \tag{2}$$

where $A(f) = 10 \log a(f)$. The noise affecting the signal has a power spectral density given by:

$$N(f) = N_t(f) + N_s(f) + N_w(f) + N_h(f) \tag{3}$$

The right hand side of Eq. 3 is the superimposition of: turbulence (t), shipping (s), wind driven waves (w), and thermal noise (h). Thus the signal-to-noise ratio (SNR) of a signal transmitted from a distance d at a frequency f is given by:

$$SNR(d,f) = \frac{P}{A(d,f)N(f)\Delta f} \tag{4}$$

where P is the power of the transmitted signal and Δf is the receiver noise bandwidth. Doppler shifts occur due to the movement of underwater nodes. The Doppler phase is a function of the relative velocity υ and the ratio between the carrier frequency and symbol rate [11]:

$$\varphi_d = -2\pi \frac{f_c}{R} \frac{\upsilon}{c-\upsilon} \tag{5}$$

where c is the speed of sound in water.

3 The Proposed System

To develop a system for wireless image transmission through a challenging channel, appropriate compression and transmission techniques should be employed. The wavelet packet decomposition is a generalization of the dyadic decomposition, where detail subbands can be further decomposed. Thus, a multitude of choices are available for image representation, and the best one with respect to the target compression efficiency can be used. SPIHT algorithm [12], provides energy compaction property, cross-subband similarity and decaying of coefficients across subbands. These properties motivated us to use wavelet packet decomposition with SPIHT for image compression (SPIHT on WP). The targets are higher energy compaction, higher coding efficiency, meanwhile preserving the

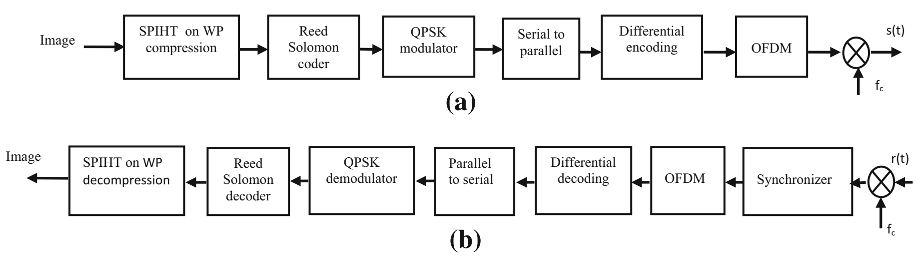

Fig. 1 System block diagram: **a** transmitter, **b** receiver

image textures, and reconstructing high quality images at the receiver under the challenging channel conditions. The system block diagram is shown in Fig. 1.

For finding the best tree of WP decomposition, the full growth approach is employed. A transform basis is adaptively selected. To compare WP basis, Shannon entropy of wavelet coefficients is used as cost function. For best basis selection, an adaptive search using single spatial tree algorithm [13, 14] is applied. The WP-based SPIHT is compared with the base-line SPIHT. Using wavelet packet decomposition, the parent–child assignments are adapted in a way that preserves the cross-level similarities. The approaches in [14–16] are used to resolve the different parental conflicts. The spatial relationship among wavelet coefficients in different subbands is defined using the spatial orientation tree structure. The significance of coefficients is predicted based on the significance of the parent coefficients.

For error detection and correction Reed–Solomon codes are used, due to their effectiveness in burst-error correction. The incorrect byte is replaced by the correct one, whether the error is caused by one or all bits. Correcting t symbols errors requires no more than $2t$ parity symbols. Improvement in error performance can be achieved by increasing the redundancy, at the expense of increased bandwidth and implementation complexity. OFDM is used to handle multipaths and to avoid complex channel equalization. By having a low bit error rate per subcarrier, the intersymbol interference (ISI) is reduced considerably. Also, by using guard intervals the ISI is reduced even more.

Errors at the receiver after the fast Fourier transform (FFT) operation may occur, thus synchronization is required. The start of the FFT window is found by correlating a reference symbol known at the receiver with the received symbols. Phase errors result from the movement of the transmitter or receiver together with carrier offset. To avoid complex carrier tracking at the receiver, and to reduce the system complexity, differential quadrature phase shift keying is used. Differential coding is done on the parallel data, since it works when there is a phase difference from two succeeding symbols from the same subcarrier.

4 Simulation Setup and Results

The proposed OFDM system for underwater wireless image transmission is simulated and tested under different channel conditions. The effects of noise, multipaths and phase errors are well investigated. For using SPIHT on WP, biorthogonal 9/7 transform is used for wavelet packets decomposition. The number of decomposition levels is 5. Fully grown tree is employed, and all possible bases are searched for best basis selection. For using SPIHT, 9/7-tap filters are used to construct five-level pyramids. Results are obtained without arithmetic coding. The performance is evaluated by analyzing the quality of the reconstructed image at the receiver versus BER. Both 0.5 and 1 bpp are used as decoding bit rates (bits per pixel).

For a given message of length $k < n$, the (n, k) Reed–Solomon codes add parity bits at the end of the message and use them to correct the errors. In this work, $n = 200$ and $k = 128$. The size of the original image is $256 \times 256 = 512 \times 128 = 65{,}536$ bytes. After adding parity bytes, the size will be $512 \times 200 = 102{,}400$ bytes. For the compressed image, the size after applying RS is $64 \times 200 = 12{,}800$ bytes with 1 bpp bit rate and $32 \times 200 = 6400$ bytes with 0.5 bpp.

The OFDM parameters used in this work are given in Table 1, and are calculated according to [17]. A base system is first designed with 8 kHz bandwidth and 1600

Table 1 OFDM parameters

Carrier frequency f_c	38 kHz		
Symbol duration T	200 ms		
Guard interval T_g	40 ms		
Subcarrier spacing $\Delta f = 1/T$	5 Hz		
Bandwidth B	8 kHz	2.56 kHz	1.28 kHz
Number of subcarriers $K = B/\Delta f$	1600	512	256
Number of symbols per subcarrier M	256	100	100
Bit rate R	13 kbps	4 kbps	2 kbps
Bandwidth utilization factor $\alpha = R/B$	1.6	1.6	1.6

subcarriers. The bandwidth is then scaled by using the same value of symbol duration and guard interval, and changing the number of subcarriers. The transmission data rate scales with the bandwidth since the utilization factor is unchanged. The total symbol time including the guard interval is 240 ms. Without compression, the total time required for transmission, including the reference symbol is 61.68 s. The bit rate is approximately 13 kbps. The total transmission time is reduced to 24.24 s with compression. This gives a bit rate of approximately 4 and 2 kbps for 1 and 0.5 bpp compression, respectively.

To simulate noise in the channel, additive white Gaussian noise (AWGN) with different signal-to-noise (S/N) ratios is added to the transmitted signal. Phase errors are simulated by multiplying the transmitted signal with $\exp(i\theta)$, where θ is the phase error, which increases from 0 to 2π during the total time of transmission. To simulate multipaths, five multipath arrivals are considered; the direct path and four delayed paths with different arrival strengths, as in Table 2. The metrics used for objective evaluation are: PSNR, WPSNR [18] and MS-SSIM [19]. With WPSNR, the contrast sensitivity function (CSF) is used to weight the spatial frequencies of a given image. MS-SSIM is used to incorporate image details at different resolutions.

Table 3 shows the effect of bit error when transmitting the original uncompressed Lena image. Table 4 shows the compressed image obtained using SPIHT and SPIHT on WP with their quality metrics. Table 7 gives the quality metrics of the decompressed image at the receiver at different values of BER. Tables 5, 6 and 8 show the quality metrics of the Dolphin image. Although the difference in quality metrics obtained using both compression techniques is slight, results show that SPIHT reconstructed images at the receiver have degraded image quality. Bits corruption may introduce significant image distortion. Errors on critical bits may lead to failure in decoding and image reconstruction. The wavelet packet transform has a no dyadic nature. This transform allows adapting the basis to the image content and to the purpose of the transformation. Applying SPIHT on WP and adapting the parent–child assignments lead to preserving the textures of the reconstructed images at the receiver and thus images with high visual quality are obtained. The sensitivity to bit errors decreases noticeably compared to SPIHT. The proposed system has an

Table 2 Amplitude and time delay of different paths

Parameter	1st path	2nd path	3rd path	4th path	5th path
Amplitude	1	0.4	0.3	0.25	0.2
Time delay (ms)	0	1	2	3	4

Table 3 Quality metrics of uncompressed Lena image at different BER values

BER	0.0009	0.001	0.01
			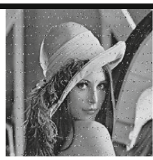
PSNR	35.0717	33.6850	23.9326
WPSNR	36.3568	36.2311	34.0908
MS-SSIM	0.99464	0.99169	0.93580

Table 4 Quality metrics of compressed Lena image using both SPIHT and SPIHT on WP

Original Lena image	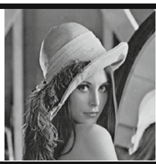	
SPIHT on WP	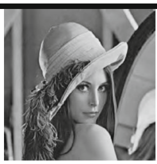 1bpp	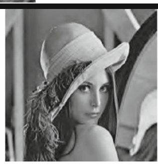 0.5bpp
PSNR	37.0258	32.1757
WPSNR	47.3856	41.2495
MS-SSIM	0.99330	0.98330
SPIHT	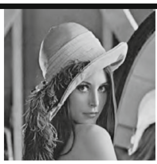 1bpp	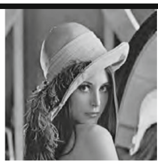 0.5bpp
PSNR	37.0540	32.2096
WPSNR	47.3900	40.5765
MS-SSIM	0.99330	0.98340

Table 5 Quality metrics of uncompressed dolphin image at different BER values

BER	0.0009	0.001	0.01
	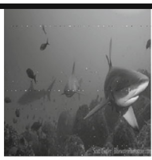	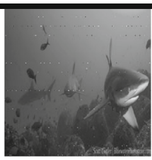	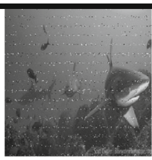
PSNR	34.7980	33.8897	24.2300
WPSNR	37.7120	36.9019	34.7193
MS-SSIM	0.98502	0.97962	0.83904

Table 6 Quality metrics of compressed dolphin image using both SPIHT and SPIHT on WP

Original Dolphin image	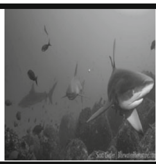	
SPIHT on WP	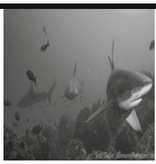 1bpp	 0.5bpp
PSNR	46.6890	41.6540
WPSNR	51.3672	51.4900
MS-SSIM	0.99800	0.99330
SPIHT	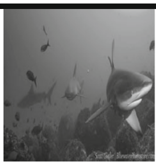 1bpp	 0.5bpp
PSNR	46.6929	41.6600
WPSNR	51.3793	51.7900
MS-SSIM	0.99800	0.99330

Table 7 Quality metrics of decompressed Lena image at the receiver at different BER values

	SPIHT on WP			SPIHT		
BER	0.0009	0.001	0.01	0.0009	0.001	0.01
1bpp	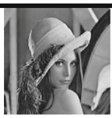	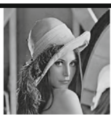	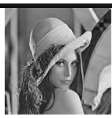	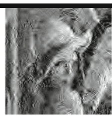	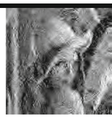	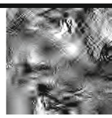
PSNR	35.6621	35.7022	29.1038	18.3713	18.3994	10.6455
WPSNR	45.4521	45.5056	34.4576	25.2485	25.3981	16.4594
MS-SSIM	0.99256	0.99262	0.97348	0.68251	0.68883	0.06850
0.5bpp	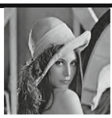	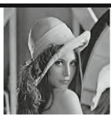	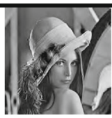		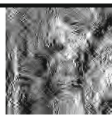	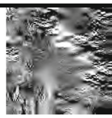
PSNR	32.0210	31.4433	24.7954	15.5727	15.1621	10.1158
WPSNR	41.0532	36.0339	30.0211	21.7488	21.6845	16.1649
MS-SSIM	0.98294	0.98213	0.89198	0.41657	0.39281	0.02814

Table 8 Quality metrics of decompressed dolphin image at the receiver at different BER values

	SPIHT on WP			SPIHT		
BER	0.0009	0.001	0.01	0.0009	0.001	0.01
1bpp			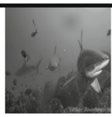	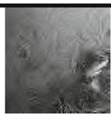	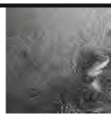	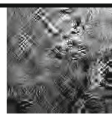
PSNR	46.0243	45.8312	37.6988	25.1369	25.4261	16.3791
WPSNR	51.2762	51.2174	41.0120	30.7405	31.0158	22.8177
MS-SSIM	0.99796	0.99781	0.9818	0.71906	0.72951	0.16284
0.5bpp				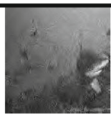	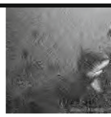	
PSNR	41.5611	40.616	37.5987	28.1865	26.5949	13.3503
WPSNR	51.3313	48.7664	39.6802	33.1434	32.3620	19.4619
MS-SSIM	0.99317	0.98731	0.97706	0.83915	0.78182	0.013869

error resilience property that curtails the severity of the damage. The execution time of applying SPIHT on WP is at least two times longer than SPIHT.

The final stages in the proposed system are smoothing and interpolation. The algorithm in [20] is applied on the received image. Smoothing is used to reduce noise while keeping the most important imprints. Interpolation is used to assign values to missing data. The algorithm uses non parametric regression. It allows robust and fast smoothing using a discrete cosine transform. The amount of smoothing is chosen by the minimization of the generalized cross-validation score. The algorithm is first applied on the received image, in

Table 9 Quality metrics of uncompressed Lena image after smoothing

BER	0.0009	0.001	0.01
	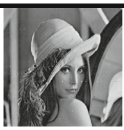	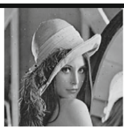	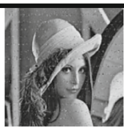
PSNR	35.9683	35.0175	28.3926
WPSNR	45.7763	47.3735	36.4957
MS-SSIM	0.99500	0.99250	0.95630

Table 10 Quality metrics of uncompressed dolphin image after smoothing

BER	0.0009	0.001	0.01
	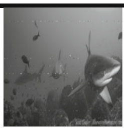	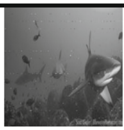	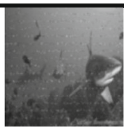
PSNR	38.0308	37.5938	32.4843
WPSNR	45.9959	44.2774	35.1855
MS-SSIM	0.98800	0.98510	0.93150

Table 11 Quality metrics of WP-based SPIHT decompressed images after smoothing

	Lena image			Dolphin image		
BER	0.0009	0.001	0.01	0.0009	0.001	0.01
1bpp	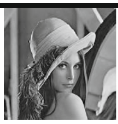	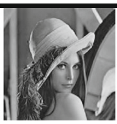	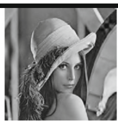	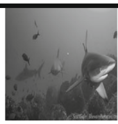	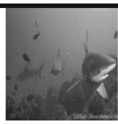	
PSNR	35.6640	35.7031	29.1050	46.0218	45.8286	37.7028
WPSNR	45.5929	45.6117	34.5033	50.8656	50.8139	41.4221
MS-SSIM	0.99260	0.99260	0.97350	0.99800	0.99780	0.98180
0.5bpp	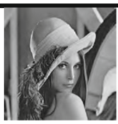	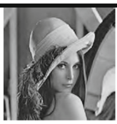		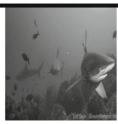		
PSNR	32.0238	31.4458	24.7966	41.5575	40.6131	37.6050
WPSNR	41.4344	36.1854	30.0504	51.3643	48.7787	39.6900
MS-SSIM	0.98290	0.98210	0.98200	0.99320	0.98730	0.97710

case of transmitting original uncompressed image. The results are given in Tables 9 and 10. Comparing with the results before smoothing (Tables 3, 5), noticeable improvement in the image quality metrics can be obtained using the smoothing technique. The effect of smoothing is also studied when transmitting WP-based SPIHT compressed images. The algorithm is applied on the decompressed images at the receiver, and the results are given in Table 11. In this case, the image quality may be slightly improved.

5 Conclusion

An efficient underwater system for wireless image transmission has been proposed. Compression is essential, and the images need to be coded within the limited bandwidth. The best tree of wavelet packet decomposition is found using the full growth approach, and SPIHT is applied on WP coefficients. The cross subband similarities have been preserved by adapting the parent–child relationships and solving the parental conflicts. For error detection and correction, Reed–Solomon has been applied. OFDM has been used with DQPSK for bit stream transmission. The SPIHT on WP and SPIHT algorithms have been compared using effective quality metrics. SPIHT results show high sensitivity to bit errors, and an uncontrolled degradation of the reconstructed quality may occur. The proposed system, on the other hand, is sufficiently error-resilient, and images can be reconstructed at the receiver with high visual quality.

References

1. Poncela, J., Aguayo, M. C., & Otero, P. (2012). Wireless underwater communications. *Wireless Personal Communications, 64*(3), 547–560.
2. Esmaiel, H., & Jiang, D. (2013). SPIHT coded image transmission over underwater acoustic channel with unequal error protection using HQAM. In *Third international conference on information science and technology, China* (pp. 1365–1371).
3. Mistry, K., & Modi, H. (2016). Design of high data rate and multipath efficient underwater acoustic communication system using OFDM–DQPSK. In *Proceedings of international conference on ICT for sustainable development, volume 408 of the series advances in intelligent systems and computing* (pp. 493–502).
4. Esmaiel, H., & Jiang, D. (2013). Image transmission over underwater acoustic environment using OFDM technique with HQAM mapper. In *Third international conference on information science and technology, China* (pp. 1596–1601).
5. Atallah, A. M., Ali, H. S., & Abdallah, M. I. (2016). An integrated system for underwater wireless image transmission. In *Proceedings of 28th International Conference on Microelectronics (ICM), Egypt* (pp. 169–172).
6. Sarisaray-Boluk, P., Gungor, V. C., Baydere, S., & Harmanci, A. E. (2011). Quality aware image transmission over underwater multimedia sensor networks. *Ad Hoc Networks, 9*(7), 1287–1301.
7. Santoso, T. B., Wirawan, & Hendrantoro, G. (2012). Image transmission with OFDM technique in underwater acoustic environment. In *7th international conference on telecommunication systems, services, and applications (TSSA), Bali* (pp. 37–41).
8. Tomasi, B., Toni, L., Casari, P., Preisig, J., & Zorzi, M. (2011). A study on the SPIHT image coding technique for underwater acoustic communications. In: *Proceedings of the 6th ACM international workshop on underwater networks*. doi:10.1145/2076569.2076578.
9. Esmaiel, H., & Jiang, D. (2014). Optimum bit rate for image transmission over underwater acoustic channel. *Journal of Electrical and Electronic Engineering, 2*(4), 64–74.
10. Urick, R. J. (1983). *Principles of underwater sound*. New York: McGraw-Hill Companies.
11. Chen, Y., Xu, X., Zhang, L., & Zou, Z. (2012). Design and application of dynamic coding in shallow water acoustic communications. In *The OCEANS, Yeosu* (pp. 1–6).

12. Said, A., & Pearlman, W. A. (1996). A new, fast, and efficient image codec based on set partitioning in hierarchical trees. *IEEE Transactions on Circuits and Systems for Video Technology, 6*(3), 243–250.
13. Ramchandran, K., Vetterli, M., & Herley, C. (1996). Wavelets, subband coding, and best bases. *Proceedings of the IEEE, 84*(4), 541–560.
14. Sprljan, N., Grgic, S., & Grgic, M. (2005). Modified SPIHT algorithm for wavelet packet image coding. *Real-Time Imaging, 11*(2005), 378–388.
15. Xiong, Z., Ramchandran, K., & Orchard, M. T. (1998). Wavelet packet image coding using space-frequency quantization. *IEEE Transactions on Image Processing, 7*(6), 892–898.
16. Rajpoot, N. M., Wilson, R. G., Meyer, F. G., & Coifman, R. R. (2003) Adaptive wavelet packet basis selection for zerotree image coding. *IEEE Transactions on Image Processing, 12*(12), 1460–1472.
17. van Nee, R., & Prasad, R. (2000). *OFDM for wireless multimedia communications*. Norwood, MA: Artech House, Inc.
18. http://www.mathworks.com/matlabcentral/fileexchange/3675-wpsnr.
19. Wang, Z., Simoncelli, E. P., & Bovik, A. C. (2003). Multis-scale structural similarity for image quality assessment. In *Proceedings of the 37th IEEE Asilomar conference of signals, systems and computers, Pacific Grove, CA* (Vol. 2, pp. 1398–1402).
20. Garcia, D. (2010). Robust smoothing of gridded data in one and higher dimensions with missing values. *Computational Statistics & Data Analysis, 54,* 1167–1178.

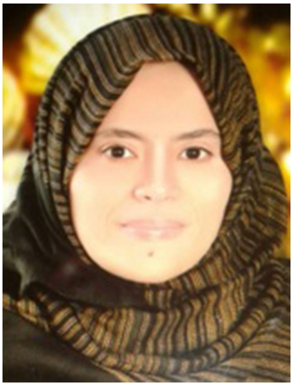

Hanaa S. Ali is an Assistant Professor in the Electronics and Communications Department, Faculty of Engineering, Zagazig University, Egypt. She is an IEEE member. She is a member in the National Committee of Radio Science in the Academy of Scientific Research and Technology (ASRT) in Egypt. She is a member in the organizing committee of the National Radio Science conference (NRSC) and has taken part in the organization of other conferences. In 2012, she received the PhD degree from Zagazig University. Her research interests include: Wireless Communication, Signal Processing, Image Processing, and Pattern Recognition. She has gained teaching experience and supervised different theses.

Asmaa M. Atallah received her B.Sc. degree in Electronics and Communication Engineering from Zagazig University, Egypt, in 2011. Her grade was very good with honors. She is currently a demonstrator in Electronics and Communication Department, Zagazig Higher Institute for Engineering and Technology, Egypt. She has studied the basics in communication and then increased her own knowledge in this area through advanced courses in the field. Her research interests are: Underwater Communication, OFDM Wireless Communication Systems, Signal Processing, and Image Processing.

M. I. Abdalla is a full professor in the Electronics and Communication Department, Faculty of Engineering, Zagazig University. He received his BSc degree from University of Mansoura, Egypt in 1979, and also the Master of Science degree from the same university in 1984. He received his PhD degree from Zagazig University, Egypt in 1989. He worked as a lecturer in Saudi Arabia from 1990 to 1993. He worked in a Post-doctoral research in University of Connecticut, USA in 1996. His research interests are Wireless communication, Signal processing, Image processing and Pattern Recognition. He has supervised different master and PhD theses. He has published many research papers in international conferences and journals.